Proceedings of the 28th IEEE
EMBS Annual International Conference
New York City, USA, Aug 30-Sept 3, 2006

The Role Restitution in Pacing Induced Spiral Wave Acceleration

Joseph V. Tranquillo, *Member, IEEE*, and Nenad Bursac

Abstract— **Attempts to terminate monomorphic tachycardia by rapid pacing occasionally lead to acceleration of the tachycardia rate followed by fibrillation. Previous experimental studies have shown that rapid pacing can convert a single-wave functional reentry into a stable multi-wave reentry with accelerated rate, but only when the single spiral rate is significantly lower than the rate the tissue can sustain. In addition the acceleration was facilitated by broad and deep conduction velocity restitution. This study explores the mechanisms that modulate the potential for and degree of acceleration. Results demonstrate that ionic changes that affect CV restitution and increase core size of the functional reentry facilitate acceleration by wave multiplication. Understanding the mechanisms for reentry acceleration may yield new strategies that prevent the degeneration of tachycardia to fibrillation.**

I. INTRODUCTION

THE transition from stable monomorphic VT to rapid polymorphic VT or VF is a life-threatening event that can result in excessive heart rate acceleration, followed by a loss of hemodynamic stability, syncope, and death [1]. A sudden burst of focal electrical activity during stable reentrant tachycardia is believed to be one of the main triggers for dangerous heart rate acceleration and the transition to fibrillation. Despite the importance of extrasystolic activations, there have been only a handful of experimental or computational studies that addressed the impact of focal activity on stable acceleration and/or break-up of a stationary reentrant wave.

In our previous studies, we optically mapped transmembrane potentials in anisotropic monolayers of neonatal rat cardiomyocytes [2-3], which, similarly to native ventricles, had dimensions smaller than the wavelength of a solitary propagating pulse. We demonstrated that bursts of point pacing often annihilated, but occasionally converted single spiral into a stable multi-wave spiral that activated the monolayer at an accelerated rate. Functional predictors for the stable acceleration were the presence of broad and deep conduction velocity (CV) restitution and a relatively large excitable gap during single spiral rotation. Furthermore, the degree of rate acceleration was proportional to the number of rotating spiral waves. It was not clear, however, if the restitution properties could dictate the formation, stability and acceleration of multi-wave spirals independent of intrinsically present microscopic structural and functional heterogeneities.

In this simulation study, we utilized a homogeneous continuous medium of a similar size to that of the cardiac monolayer to study the role of restitution in the formation and stability of multi-wave spirals. Our simulations show that, similar to experimental studies, appropriately timed point stimuli can induce stable accelerated multi-wave spirals only in media with a relatively large excitable gap. Furthermore, changes in only the action potential duration (APD) restitution did not result in stable rate acceleration. In contrast, changes in CV restitution, caused by a change in the onset or recovery of fast depolarizing currents, dictated the size of the excitable gap and degree of rate acceleration in multi-wave spirals.

II. METHODS

A. *Dynamic Restitutions*

The Fenton-Karma (FK) simplified ionic model [4], was used for all studies and consists of: 1) a fast inward (I_{fi}) that mimics the sodium currents, 2) a slow inward (I_{si}) that mimics calcium currents and 3) a slow outward (I_{so}) that mimics potassium currents. Simulations [5] in a 2cm one-dimensional (1D) cable (σ=1mS/cm Δx=0.01cm finite difference, Δt=4μs explicit Euler) were conducted to derive dynamic action potential duration (APD) and conduction velocity (CV) restitution curves [6]. Six, 2X-threshold stimuli were applied to x=0cm at increasing rates from 1Hz to 10Hz in increments of 0.25Hz. Since the FK model has limited memory, the CV and APD of the sixth action potential at each pacing rate was used for analysis. The APD was measured at x=1cm as the time between the fastest upstroke ($\dot{V}_{max}$) and 80% repolarization of the action potential. Conduction velocities were measured using the delay between $\dot{V}_{max}$ at x=0.5 cm and x=1.5 cm. APD and CV were plotted against the *cycle length* (CL, inverse of the pacing rate). The smallest cycle length that propagated action potentials in a 1:1 fashion (the leftmost point on the restitution curve) was defined as the *minimum cycle length* (MCL).

The magnitude, and timing of activation and inactivation of the three currents in the FK model were adjusted to approximate the experimentally measured APD and CV restitution from our previous studies in monolayers of neonatal rat ventricular cells [2-3]. From the NPS, all parameters were independently varied over a range of values and their effects on single spiral dynamics were examined in a simulated 2D sheet.

Manuscript received April 3, 2006. This work was supported in part by the U.S. Department of Commerce under Grant BS123456 (sponsor and financial support acknowledgment goes here) and

J.V. Tranquillo is with the Bucknell University Biomedical Engineering Program, Lewisburg, PA 17837 USA (email:jvt002@bucknell.edu; phone: 570-577-1758).

N. Bursac is with the Duke University Biomedical Engineering Department, Durham, NC 27708 USA (e-mail:nbursac@duke.edu phone: 919-660-5510).

B. *Single Spiral Analysis*

A single spiral was initiated in a uniform 2D tissue sheet (2cmx2cm, σ=1mS/cm, Δx=0.01cm, Δt=4μs, finite difference semi-implicit Crank-Nicholson) using a cross-field S1-S2 protocol. Once a spiral was initiated, ten seconds were elapsed to ensure stability and enable the spiral to reach a constant position and rotation rate. A further 20 seconds of spiral activity was simulated, during which the average time interval between successive $\dot{V}_{max}$ was computed for tissue nodes along the border of the 2-D sheet. The average period at which a spiral stimulated this remote tissue was named the *spiral cycle length* (SCL). All 2D simulations were run on 16 processors of either the Duke University High Performance Computing Cluster or the Pittsburgh Supercomputing Center.

C. *Potential for Acceleration*

As shown in our previous experimental studies, the ability to multiply and accelerate a single spiral was associated with relatively large values of: 1) ΔCL, measured as the difference between spiral CL and minimum CL (i.e., ΔCL=SCL-MCL), and 2) ΔWL, measured from the WL restitution as ΔWL=WL(SCL)-WL(MCL). The ΔCL and ΔWL, descriptors of the temporal and spatial excitable gap of a spiral wave, respectively, defined the potential for spiral rate acceleration and wave multiplication. FK parameters that independently yielded high values of ΔCL (>10msec) and ΔWL (>0.2 cm) were used to study the induction of stable multi-wave spirals and possible rate acceleration.

Spiral wave dynamics were assessed using phase map analysis as previously described [7]. The movement of a phase singularity (PS) was tracked from one time step to the next to create a map of spiral tip motion over time To characterize the meander of the spiral tip, we measured a "PS pathlength", defined as the distance (in mm) that the PS transverses during one rotation of the spiral, and a "PS velocity", defined as the average velocity of PS motion (in cm/s) over 10-20s of the spiral rotation.

D. *Multi-Spiral Analysis*

To initiate a multi-wave spiral, an appropriately timed S3 point stimulus was delivered in the wake (e.g. repolarization tail) of a single spiral wave. The S3 stimulus resulted in a wavebreak and formation of two new spirals (i.e. 2 new PSs). The interaction between these two new PS and the initial PS eventually yielded one of the following cases: 1) termination of all activity, 2) no change in the number of spiral waves in the tissue sheet, or 3) stable spiral multiplication. If stable multi-spiral pattern was formed (i.e. persisted for 20 s), an S4 point stimulus was applied at the same or a different site in an attempt to further increase the number of stably rotating waves.

Similar to our previous studies, multi-wave spirals were classified according to the number and chirality (direction of rotation) of stably rotating spiral waves. For example, a single spiral was assigned type 1/0 for having 1 stable PS of one chirality and 0 of the opposite chirality. A figure-of-eight spiral was assigned type 1/1 since it has 2 stable counter-rotating waves (with (+) and (-) chirality). Similarly, a two-arm spiral was assigned type 2/0. To assess the dynamics of multiple stable spiral tips, the PS tracking analysis described above was performed for each spiral during 20s of activity. Likewise, the PS pathlength and PS velocity were calculated for each spiral tip and averaged among the tips.

Analogous to the single spiral CL, the average period at which a multi-wave spiral activated the periphery of the 2D tissue sheet was named the Multi-Spiral Cycle Length (MSCL). The relative increase of the multi-wave spiral rate compared to the single spiral rate (with the same membrane properties) was defined as the percent acceleration (%Accel = 100*(SCL-MSCL)/MSCL). The ΔCL for multi-wave spiral was computed as ΔCL=MSCL-MCL.

III. RESULTS

A. *Nominal Parameter Set (NPS)*

FK parameters were found that approximated the experimental APD and CV restitution curves. At a basic pacing CL of 500 ms, the CV and APD were 29.8cm/s and 165.8msec, respectively, yielding a WL of 4.9cm which was significantly larger than the dimensions of the medium. The minimum cycle length (MCL) was 148msec, while the spiral cycle length (SCL) was 155msec. Therefore, the spiral was rotating at a period 7msec slower (ΔCL = SCL-MCL= 7ms) than what could be sustained in the same tissue excited by a planar wave. The PS pathlength and velocity for the nominal single spiral were 0.2mm/cycle and 0.13cm/s respectively.

B. *Single Spiral Analysis*

Parameters of the FK model were independently varied around the NPS in order to alter APD and CV restitution, and study the resulting changes in single spiral behavior. Three parameters of the FK model (τ_{v1}, τ_0 and g_{fi}) were identified for which changes yielded ΔCL>10msec and ΔWL>0.2cm. These parameters were then used for studies of spiral acceleration. A fourth parameter, I_{so} (amplitude of slow outward current), was also studied because, unlike the other 3 parameters, it had significant effects only on APD, but not on CV restitution. For all of the parameter combinations, the maxim slope of APD restitution (as a function of diastolic interval) was <1 and no APD alternans were present, similar to our studies in neonatal rat cardiac monolayers [2-3].

The recovery time constant of the fast inward current (τ_{v1}) was varied between 20 and 1000, with 30 being the nominal value. Physically, increasing τ_{v1} slows down inactivation of the fast inward current (comparable to Na current). Consequently, the available fast inward current is decreased at lower, but not at higher pacing CLs. Increased τ_{v1} resulted in increased MCL as well as steepened APD and

particularly CV restitution. Furthermore, with increased τ_{v1}, the SCL increased faster than the MCL, yielding an increase in ΔCL to a maximum value of 44 ms for τ_{v1}=100 (Table 1). Similarly, ΔWL increased with increased τ_{v1}. Finally, increasing τ_{v1} resulted in a higher degree of meandering of the spiral tip as well as increased PS pathlength and velocity as compared to the nominal case.

The time constant of the onset of the slow outward current (τ_0) was varied between 1.5 and 8, with 6 being the nominal value. Physically, decreasing τ_0 speeds up the onset of outward current (comparable to K currents), which counteracts the depolarization process. Consequently, the threshold for an action potential initiation was higher and the total current during late depolarization was lower for all pacing CLs. Decreased τ_0 resulted in no change in MCL or APD restitution. CV restitution, however, was lower at all CLs (without significantly changing the restitution slope). Although MCL did not change with decreased τ_0, the SCL increased, yielding an increased ΔCL to a maximum value of 61 ms for τ_0=1.5 (Table 1). The ΔWL also increased with increased τ_0. Similar to τ_{v1}, decreased τ_0 induced increased meandering of the spiral tip with increased PS pathlength and PS velocity.

Maximum conductivity of the fast inward current (g_{fi}) was varied between 0.8 and 5, with 3 being the nominal value. Physically, decreasing g_{fi} decreases the fast inward current (comparable to Na current) and reduces excitability of the medium. Decreased g_{fi} resulted in slightly decreased MCL, and significantly decreased APD and CV for all CLs. Consequently, the maximum restitution slopes decreased. Furthermore, while MCL slightly decreased with decreased g_{fi}, the SCL increased, yielding an increase in ΔCL to a maximum value of 98ms for g_{fi} =0.8. Similar to τ_{v1} and τ_0, the decrease in g_{fi} resulted in increase in ΔWL. The spiral tip exhibited a high degree of meandering, and an increase in PS pathlength, and velocity.

The amplitude of the slow outward current (I_{so}) was varied between 85% and 120% of its nominal value. Physically, decreasing $\%I_{so}$ (comparable to K currents) impedes repolarization and prolongs the APD, but has negligible effect on depolarization of the action potential. Decreased $\%I_{so}$ resulted in a slightly increased MCL, steeper APD restitution, but no change in CV restitution. Furthermore, SCL and MCL were similarly affected by changes in %Iso, yielding only negligible changes in ΔCL and ΔWL. The spiral tip meandering on the other hand, as well as average PS pathlength and velocity, did increase as the $\%I_{so}$ amplitude was decreased.

C. *Multi-Spiral Analysis*

The four media (τ_{v1}=100, τ_0=1.5, g_{fi}=0.8 and $\%I_{so}$=85%) were used to study cases of stable 1/1, 2/0, and 2/1 multi-wave spirals (Table 1). In all 12 cases, individual spiral waves in a multi-wave pattern were mutually entrained and therefore rotated at the same rates. Adjacent waves merged for a period of time along their common pathways, an event that occurred once per rotation and promoted the synchronization of the period and phase among different regions in the tissue. Phase map plots with PS (spiral tip) trajectories during 20 seconds of activity are shown in Figure 1.

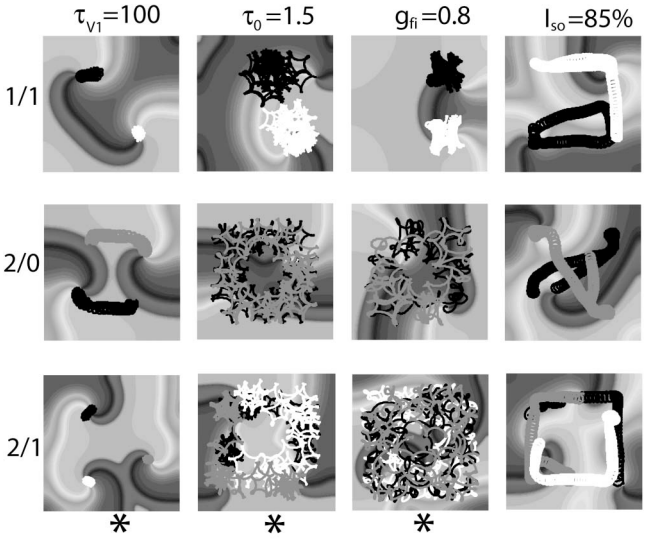

Fig 1. Phase singularity trajectories for different multi-wave spirals. Columns and rows denote parameter values and spiral types, respectively. Black and gray colors denote PSs with positive chirality, while white color denotes PSs with negative chirality. PS trajectories are depicted during a 20s interval. All tissue sizes are 2cm x 2cm, except for those denoted by (*) which represent a 3cm x 3cm tissue.

The PSs exhibited a variety of complex motions with trajectories that were found to be either separated and relatively stationary (for τ_{v1}) or drifting and overlapping (for τ_0, g_{fi}, and $\%I_{so}$). The PSs exhibited either unconstrained, continuous meandering around each other (e.g. 2/0 cases for τ_{v1}, τ_0, and g_{fi}, or 2/1 case for g_{fi}) as well as localized "clustering" with occasional escapes (e.g. 2/1 case for τ_0), similar to experiments in monolayers of neonatal rat cardiomyocytes [2-3].

The pacing-induced conversion of single to multi-wave spirals resulted in acceleration for τ_{v1}=100, τ_0=1.5, and g_{fi}=0.8 but not for $\%I_{so}$=85%. Consequently, the period of activation during accelerated multi-wave spirals approached the minimum sustainable CL during planar wave excitation (i.e. ΔCLs decreased). In general, for each of the three accelerated cases (τ_{v1}, τ_0, and g_{fi}), the rate of activation due to spiral wave activity followed the inequality: spiral rate of 1/0 < 1/1 < 2/0 < 2/1, similar to findings in neonatal rat monolayers. It should be noted, however, that stable 2/1 spiral was not attainable for τ_{v1}=100 and g_{fi}=0.8 in the 2cmx2cm medium. To obtain data for these cases, the size of the medium was increased to 3cmx3cm. The highest acceleration of 17.3% (ΔCL=12ms) during a 2/1 spiral was observed for τ_{V1}=100. Furthermore a stable 2/2 spiral for τ_{v1}=100 also induced in a 3cm x 3cm medium (with 4

spatially separate PS trajectories, not shown), exhibited 21.9% acceleration (ΔCL=6 msec), further supporting the finding that the degree of acceleration was directly correlated with the number of rotating waves. The limit in the rate acceleration is achieved when MSCL approached MCL (i.e. for small ΔCL and ΔWL) beyond which further acceleration is not possible.

TABLE 1
Characterization of single and multi-wave reentries

	CL	ΔCL	%A	PL	V
1/0					
τ_{V1}=100	210	44	--	2.9	1.38
τ_0=1.5	214	61	--	5.6	2.61
g_{fi}=0.8	240	98	--	28.2	11.75
%I_{so}=85%	160	0	--	2.8	1.75
1/1					
τ_{V1}=100	191	25	9.9	3.0	1.57
τ_0=1.5	208	55	2.9	7.1	3.41
g_{fi}=0.8	218	76	10.1	20.3	9.31
%I_{so}=85%	160	0	0	2.9	1.80
2/0					
τ_{V1}=100	189	23	11.1	3.1	1.64
τ_0=1.5	205	52	4.4	6.2	3.02
g_{fi}=0.8	220	78	9.1	25.2	11.45
%I_{so}=85%	160	0	0	3.3	2.04
2/1					
τ_{V1}=100 (*)	179	12	17.3	2.4	1.34
τ_0=1.5 (*)	187	34	14.4	12.4	6.63
g_{fi}=0.8 (*)	208	66	15.4	22.2	10.7
%I_{so}=85%	160	0	0	3.1	1.95

CL(msec), ΔCL(msec), %A (%acceleration), PL (PS Pathlength in mm/cycle) and V (PS Velocity in cm/s). *data obtained in a 3cm x 3cm tissue sheet.

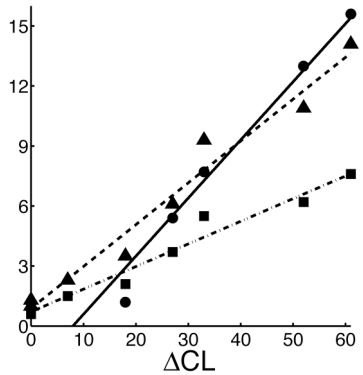

Fig 2. Correlation between DCL and %Acceleration (circle, solid line), PS Pathlength (triangle, dashed line) and PS Velocity (square, dash-dot line).

To determine the correlation between ΔCL and spiral characteristics, the 2/1, τ_0=1.5 reentry was slowly decelerated by incrementally increasing τ_0 from 1.5 to 8. Good correlation was found (Figure 2) between ΔCL and %Acceleration, PS velocity and PS pathlength. Correlation coefficients for %acceleration, PS velocity and PS pathlength were 0.986, 0.970 and 0.965 respectively.

IV. DISCUSSION

In summary, the parameters that changed both CV and APD restitution (g_{fi} and τ_{v1}), or CV restitution only (τ_0), but not APD restitution only (I_{so}), significantly increased ΔCL providing a necessary condition for spiral rate acceleration. The decrease in sodium conductance (g_{fi}) reduced available sodium depolarizing current at all pacing CLs, while τ_{v1} directly decreased available depolarizing current only at high CLs. On the other hand, τ_0 indirectly reduced available depolarizing current at all CLs by modulating the beginning of repolarization. These alterations resulted in changed kinetics of the reentrant wavefront and an increase in the meander of the spiral tip and size of the excitable gap, as well as provided conditions for reentry acceleration. Consequently, our data suggest that patients treated with class Ia antiarrhythmic agents (e.g. disopyramide, cibenzoline) may have increased chances of reentry acceleration during antitachycardia pacing. Conversely, class III agents (potassium channels blockers) are not expected to alter excitable gap and thus affect incidence of acceleration [8]. Table 1 indicates that the meander of the single spiral (as measured by the velocity) was a reasonable predictor of ΔCL. For example, the g_{fi} spiral meanders the most and also has the largest ΔCL.

REFERENCES

[1] A.M. Katz, "Physiology of the heart," 2nd ed. New York: Raven Press, 1992, pp 515-517.

[2] N. Bursac, L. Tung, "Acceleration of function reentry by rapid pacing in anisotropic cardiac monolayers: formation of multi-wave function reentries," *Cardiovasc Res.* vol 69,2 pp381-90. 2006.

[3] N. Bursac, F. Aguel, L. Tung, "Multiarm spirals in a two-dimensional cardiac substrate," *Proc Natl Acad Sci.* vol 101, 43 pp 15530-4.

[4] F.H. Fenton, A. Karma, "Vortex dynamics in three-dimnesional continuous myocardium with fiber rotation: Filament instability and fibrillation," *Chaos.* vol 879, 4 pp 20-47. 1998.

[5] J.B. Pormann, "A modular simulation system for the bidomain equations," PhD. Thesis Duke University Department of Electrical and Computer Engineering. 1999.

[6] M.L. Killer, M.L. Riccio, R.F. Gilmour, "Dynamic restitution of action potential duration during electrical alternans and ventricular fibrillation," *Am J Physiol.* vol 275,5 pp H1635-42. 1998.

[7] R.A. Gray, A.M Pertsov, J. Jalife, "Spatial and temporal organization during cardiac fibrillation," *Nature.* vol 392, 6671 pp 20-1. 1998.

[8] Z. Qu, J.N Weiss, "Effects of Na+ and K+ channel blockade on vulnerability to termination of fibrillation in simulated normal cardiac tissue," *Am J Physiol.* vol 289,4 pp H1692-701. 2005.